

A 4 x 8-Gbps VCSEL Array Driver ASIC and Integration with a Custom Array Transmitter Module for the LHC Front-end Transmission

Di Guo^{a,b,*}, Chonghan Liu^a, Jinghong Chen^c, John Chramowicz^d, Datao Gong^a,
Huiqin He^{a,e}, Suen Hou^f, Tiankuan Liu^a, Alan Prosser^d, Ping-Kun Teng^f,
Annie C. Xiang^a, Le Xiao^{a,g} and Jingbo Ye^a

^a Department of Physics, Southern Methodist University, Dallas, TX 75275, USA

^b State Key Laboratory of Particle Detection and Electronics, University of Science and Technology of China, Hefei Anhui 230026, China

^c Department of Electrical and Computer Engineering, University of Houston, Houston, TX 77004, USA

^d Real-Time Systems Engineering Department, Fermi National Laboratory, Batavia, IL 60510, USA

^e Shenzhen Polytechnic, Shenzhen 518055, P.R. China

^f Institute of Physics, Academia Sinica, Nangang 11529, Taipei, Taiwan

^g Department of Physics, Central China Normal University, Wuhan, Hubei 430079, P.R. China

Abstract

This paper describes the design, fabrication and experiment results of a 4 x 8-Gbps Vertical-Cavity Surface-Emitting Laser (VCSEL) array driver ASIC with the adjustable active-shunt peaking technique and the novel balanced output structure under the Silicon-on-Sapphire (SOS) process, and a custom array optical transmitter module, featuring a compact size of 10 mm x 15 mm x 5.3 mm. Both the array driver ASIC and the module have been fully tested after integration as a complete parallel transmitter. Optical eye diagram of each channel passes the eye mask at 8 Gbps/ch with adjacent channel working simultaneously with a power consumption of 150 mW/ch. The optical transmission of Bit-Error Rate (BER) less than 10E-12 is achieved at an aggregated data rate of 4 x 8-Gbps.

Keywords: Optical detector readout concepts; Front-end electronics for detector readout; Lasers Driver ASIC; Array optical transmission

1. Introduction

VCSEL-based parallel optical data links have recently seen rapid and wide-spread deployment in high performance computing labs, data centers and Ethernet networks. The benefits include highly aggregated bandwidth, compact footprint and low power consumption. To apply the parallel optical links to the LHC upgrades as well as in other collider detector developments [1], these devices have to meet rigid environmental demands of radiation, electro-magnetic field, temperature and volume size. The high luminosity running of the LHC (HL-LHC), with instantaneous luminosities of $5 \times 10^{34} \text{ cm}^{-2} \text{ s}^{-1}$ and an integrated luminosity of 3000 fb^{-1} , for example, will request that the opto-electronics devices are close to the beam pipe to withstand integrated radiation dose of 100KGy and 10^{15} neutrons/cm² [2, 3].

Two critical developments, the array driver ASIC and the array optical coupling, are indispensable towards a dedicated array optical transmitter for on-detector deployment. Prior developments on single channel optical transceivers, such as CERN's versatile link project [4], have successfully qualified commercial components, custom developed OE circuitry and assembly packages. In advancing to array-based parallel modules, limited by the channel-to-channel pitch of extremely tight industrial standard, both the array ASICs and the array optical module face new customization challenges.

A family of data link ASICs has been developed by SMU using a commercial 0.25- μm Silicon-on-Sapphire (SOS) CMOS technology [5]. The LOClD4 ASIC is a four channel, 8-Gbps/ch laser array driver designed for the array optical transmitter module. Each channel receives the low-swing Current-Mode Logic (CML) signal (200 mV differential peak-to-peak), outputs a modulation-current signal of 7.5 mA with an average current of 6.25 mA with a power consumption of 150 mW/ch at 8 Gbps/ch. This is the first VCSEL array driver ever fabricated at this aggregated bandwidth targeting high-energy physics experiments. Programmable active-shunt peaking technique is used to extend the bandwidth in pre-driving stages [6]. A novel structure of the output

stage removes the ordinary extra bias-circuit, and delivers both bias and modulation current with balanced branches to effectively minimize the noise and crosstalk from the power supply.

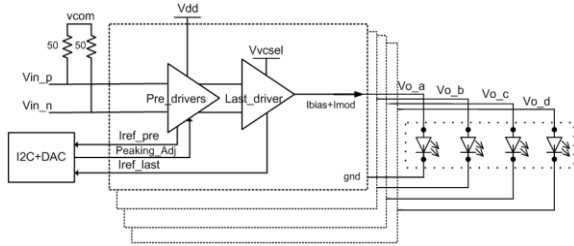
After integrated within a custom array optical transmitter (ATx), the LOClD4 is able to be fully tested. The ATx module, while utilizing generic commercial array-optical-coupling components [7], is assembled via a custom low-cost reliable active-alignment procedure. Radiation tolerance has been tested at individual component level. The commercial VCSEL arrays (12-channel GaAs quantum well surface emitter) are being surveyed continuously with quantitative Non-Ionizing Energy Loss (NIEL) up to 10^{15} cm^{-2} 1-MeV neutrons equivalents by CERN [8]. The commercial array optical elements have been exposed to x-ray up to 96 Mrad(SiO₂) at a dose rate of 6668 Krad(SiO₂)/hr, no radiation-induced attenuation is observed [9]. The radiation tolerant performance of the SOS process has been evaluated [10], and verified on a single channel VCSEL driver with x-ray and high-energy neutron beam test [11].

The structure and design of the four-channel VCSEL Array driver LOClD4 are discussed in Section 2. The array transmitter module development and optical alignment procedures are described in Section 3. In Section 4, we discuss the full-channel optical test of the LOClD4 after integration with the ATx module. And the conclusions are presented in Section 5.

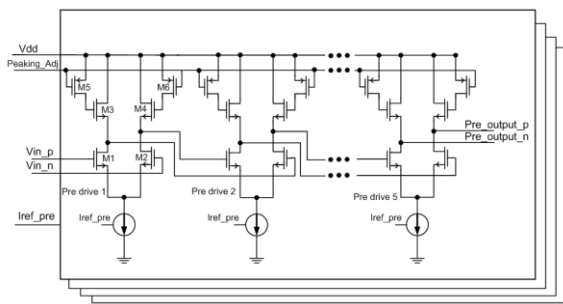
2. Four-channel VCSEL Array driver: LOClD4

The block diagram of LOClD4 is shown in Fig. 1. A common voltage (vcom) of 1.9 V is provided internally with impedance match as the input interface, followed by the pre-drivers with the 3.3 V (Vdd) power supply and the last output driver with the 3.8 V (Vvcsel) power supply. The pre-drivers are five-stage differential amplifiers with the adjustable active-shunt peaking technique for the consideration of amplification and bandwidth. The peaking strength and the tail current of pre-drivers, which mainly controls the modulation amplitude, are both adjustable through the Peaking_Adj and the Iref_pre respectively, as shown in the Fig. 1.

90 The last driver, receiving the differential outputs
 91 of pre-drivers, adopts the single-end, open-drain



92
 93
 94 Fig. 1. Block diagram of the 4-channel array driver LOClD4



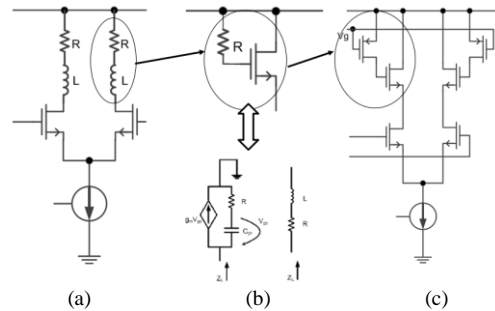
95
 96
 97 Fig. 2. Schematic of the pre-drivers in the LOClD4

98
 99 structure to enable the DC coupling between the
 100 VCSEL and the driver for the array application. It
 101 combines the supply of bias and modulation current
 102 without the conventional extra bias-current circuit,
 103 and deliberately designs the load of internal branch to
 104 match with the external branch (VCSEL load). This
 105 novel “balanced” structure effectively weakens
 106 switching components on the power supply of the last
 107 driver, which minimize the ground bounce noise and
 108 crosstalk accordingly when compared to the
 109 conventional single-end output stage.

110 2.1. Adjustable active-shunt peaking technique in 111 pre-driver designs

112 For the radiation-tolerant purpose and as a
 113 member of the data link ASIC series, the LOClD4
 114 adopts the Silicon-on-Sapphire process. However, the
 115 bandwidth is significantly restricted by the transit
 116 frequency of this 0.25- μm CMOS process. To offset
 117 the bandwidth disadvantage, multi-stage
 118 amplification and an adjustable active-shunt peaking

119 technique based on the regular inductance peaking
 120 are used in pre-drivers, as shown in Fig. 2. The pre-

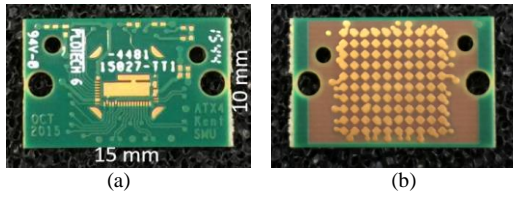


121
 122
 123 Fig. 3. (a) Passive inductance peaking, (b) Active shunt peaking
 124 (c) Adjustable active-shunt peaking used in the LOClD4

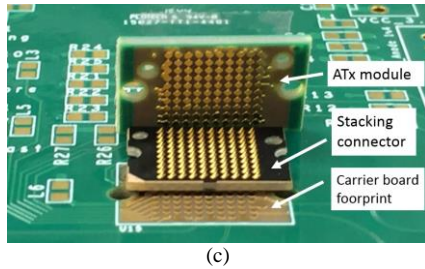
125
 126 drivers of each channel consist of five DC-coupled
 127 stages with active loads. All these differential stages
 128 between different channels share the same 1.2 V
 129 (Vdd) power source within the chip.

130 The inductive load added to the drain, the so-
 131 called shunt peaking technique, is a conventional and
 132 widely-used way to boost the bandwidth [12]. It
 133 creates one more pole in the transmission equation of
 134 the common-source amplifier to broaden the
 135 bandwidth, as shown in Fig. 3(a). But the passive
 136 inductance generally costs a large chip area.
 137 Moreover, for the array driver application, the area of
 138 the single channel is rigidly restricted by the VCSEL
 139 Array, which has a fixed channel-to-channel interval
 140 of 250 μm . It makes the passive inductance
 141 completely unaffordable under the SOS process. The
 142 active-shunt peaking [13], as shown in Fig. 3(b), is an
 143 alternative method for the area-saving consideration.
 144 The resistor R, the capacitance between source and
 145 gate, and the V_{gs} -controlled I_{ds} consist of an active
 146 inductance with both equivalent conductive and
 147 resistive loads. Further, the resistor R in Fig. 3(b) can
 148 be substituted by a PMOS, which acts as a voltage-
 149 controlled resistor. The final structure is shown in
 150 Fig. 3(c). The PMOS gate voltage controls the value
 151 of the resistance, changes the equivalent value of the
 152 inductance, and makes the peaking strength
 153 adjustable consequently. The programmable structure
 154 enables the bandwidth optimization for each chip
 155 under applications of different bit rates, and also
 156 solves the instability problems of practical resistance
 157 value in the process.

229
230

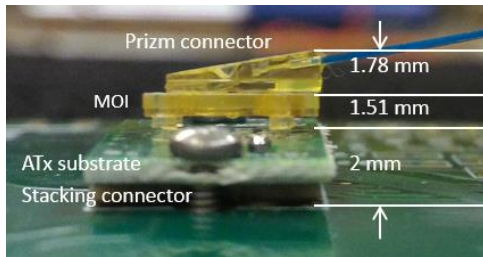


231
232



233 Fig. 7. Electrical interface of the ATx module: (a) ATx substrate
234 top, (b) ATx substrate bottom, (c) stacking structure

235



236
237

238 Fig. 8. Fully assembled ATx module on the carrier board

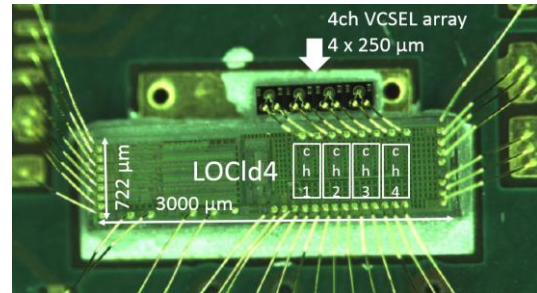
239

240 under 1 dB, and below -50 dBm respectively [9].

241 3.1. Electrical interface

242 A number of electrical interface variants have
243 been designed for different optimization purposes.
244 The first ATx prototype utilizes peripheral half-via
245 structures that can be directly soldered onto carrier
246 board. Both FR4 Print Circuited Board (PCB) and
247 Alumina ceramic substrates have been used and both
248 demonstrated sufficient transmission signal integrity
249 [14]. With the latest high-speed ultra-low profile
250 stacking connector [15], the electrical interface is
251 updated to a pluggable version with the footprint
252 further reduced from 19 mm x 22 mm to 10 mm x 15
253 mm.

254 Fig. 7(a) (b) shows the top and bottom sides of the



255

256

257 Fig. 9. LOClD4 and VCSEL array die attached and bonded

258

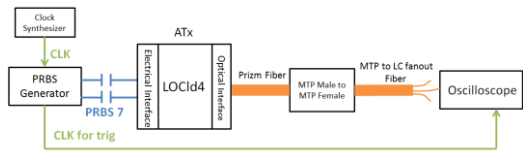
259 ATx substrate. The VCSEL array die and the driver
260 die will be mounted on the top side of the substrate
261 with the MOI assembled above. The bottom of the
262 substrate adopts a footprint similar to the ball grid
263 array (BGA) package with a pitch of 0.8 mm. The
264 stacking connector, shown in Fig. 7(c), serves as a
265 spacer between the ATx and the carrier board. Metal
266 compression contacts are arranged at both sides of
267 the connector to offer the top-to-bottom electrical
268 connection. These contacts are corresponding to both
269 the substrate footprint and the carrier board footprint.
270 Fig. 7(c) shows the overall structure of the electrical
271 interface.

272 The ATx module will be finally fixed onto the
273 carrier board together with the stacking connector
274 using two guide pins for positioning and two precise
275 screws for mechanical reinforce. Fig. 8 shows a
276 complete ATx module assembled on the carrier
277 board. The total height of the ATx module in
278 application is less than 5.3 mm.

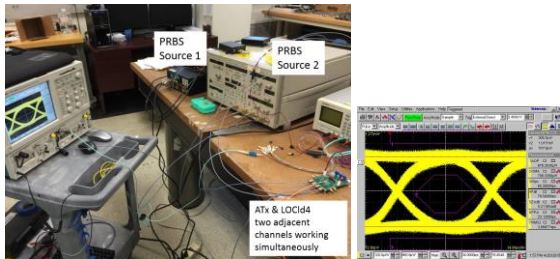
279 4. Full-channel optical test of the LOClD4 after 280 integration with the ATx module

281 With the custom array module ATx and the
282 active-alignment method, the array driver LOClD4 is
283 able to be integrated within the module and fully
284 evaluated. Fig. 9 is a photo of the LOClD4 and the 4-
285 ch ULM 14G VCSEL array [16] dies attached and
286 wire-bonded on the ATx substrate.

287 Fig. 10(a) (b) shows the block diagram and the
288 setup picture of the optical eye diagram test. During
289 the test, two pseudo random binary sequence (PRBS)



(a) Block diagram of the optical eye test



(a) Picture of the test setup

(b) 5 Gbps eye diagram

Fig. 10. Optical eye diagram test setup and a 5 Gbps optical eye

generators were used with independent data patterns and clock sources to take into account the multi-channel crosstalk. The amplitude of the PRBS signals was set to differential peak-to-peak 200 mV. At the peaking strength of 2.2 V, an optimum 5 Gbps optical eye diagram was captured as shown in the Fig. 10(c), when adjacent channel working simultaneously at 5 Gbps.

Fig. 11 shows the optimum 8 Gbps optical eye diagrams at a peaking strength of 2.4 V. All four channels were recorded when adjacent channel working simultaneously at 8 Gbps, and passed the eye mask test without a single violation.

Another BER link test was also conducted. The commercial SFP+ module was used as the receiver, and the LOCId4+ATx worked as the transmitter. The optical output of each channel was received by the SFP+ and verified with the PRBS 7 pattern. Every channel was tested at 5 Gbps and 8 Gbps with a total bits up to $5E12$, and not a single error was found. BER less than $10E-12$ was achieved at each channel at the rate of 5 Gbps and 8 Gbps when adjacent channel working at the same bit rate.

5. Conclusion

We have reported the development of a fabricated VCSEL array driver ASIC and a parallel optical transmitter module using commercial array optical

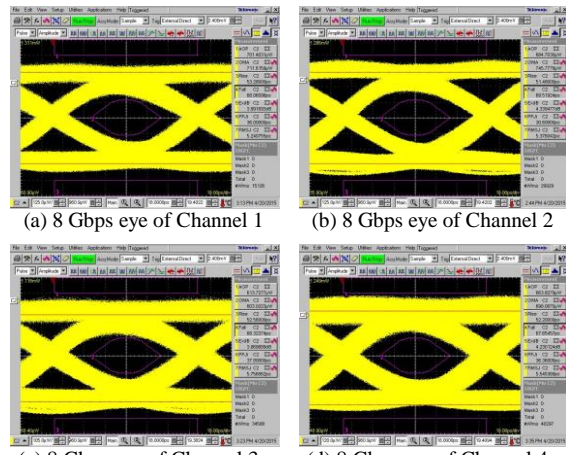


Fig. 11. Optical eye diagrams of all four channels at 8 Gbps

components. The array driver has been integrated within the array module, and optically tested as a complete parallel optical transmitter that supports 4 x 8-Gbps data transmission. All four channels pass the optical eye-diagram mask test at the rate of 8-Gbps/ch when adjacent channel working simultaneously with a power consumption of 150 mW per channel (VCSEL power included). The BER less than $10E-12$ transmission is achieved.

Acknowledgments

This work is supported by the US Department of Energy Collider Detector Research and Development (CDRD) data link program. The authors also would like to thank Jee Libres of VLISP, Alan G Prosser of Fermi Lab, Michael Wiesner of ULM and Alan Ugolini of US Conec for informative discussions.

References

- [1] J. Chramowicz et al., Evaluation of emerging parallel optical link technology for high energy physics, 2012 JINST 7 C01007.
- [2] ATLAS Collaboration, ATLAS liquid argon calorimeter phase-I upgrade technical design report, CERN-LHCC-2013-017, ATLAS-TDR-022, September 2013.
- [3] ATLAS Collaboration, Letter of Intent Phase-II Upgrade, CERN-2012-022, LHCC-I-023, December, 2012.

- 354 [4] L. Amaral, S. Dris, A. Gerardin, T. Huffman, C. Issever, A.J.
355 Pacheco et al., The versatile link, a common project for super-
356 LHC, Journal of Instrumentation, 2009 JISNT 4 P12003.
- 357 [5] L. Xiaoting et al., Optical Data Transmission ASICs for the
358 High-Luminosity LHC (HL-LHC) Experiments, Journal of
359 Instrumentation, 2014 JINST 9 C03007.
- 360 [6] F. Liang et al., The Design of 8-Gbps VCSEL Drivers for
361 ATLAS Liquid Argon Calorimeter Upgrade, Journal of
362 Instrumentation, 2013 JINST E02001.
- 363 [7] D. Childers et al., Miniature detachable photonic turn
364 Connector for Optical Module Interface, 61st IEEE Electronic
365 Components and Technology Conference (ECTC), 2011, pp.
366 1922-1927.
- 367 [8] J. Troska et al., Radiation damage studies of lasers and
368 photodiodes for use in Multi-Gb/s optical data links, IEEE
369 Transactions on Nuclear Science, VOL. 58, No. 6, December
370 2011.
- 371 [9] D. Guo et al., The VCSEL-based array optical transmitter
372 (ATx) development towards 120-Gbps link for collider
373 detector: development update, Journal of Instrumentation,
374 2015 JINST 10 C01034.
- 375 [10] T. Liu et al., Total Ionization Dose Effects and Single-Event
376 Effects Studies of a 0.25 μm Silicon-On-Sapphire CMOS
377 technology, at 9th European Conference on Radiation and Its
378 Effects on Components and Systems, RADECS 2007,
379 Deauville France (2007).
- 380 [11] X. Li et al., 8-Gbps-per-channel radiation-tolerant VCSEL
381 drivers for the LHC detector upgrade, Journal of
382 Instrumentation, 2015 JINST 10 C02017.
- 383 [12] T. Lee, The Design of CMOS Radio-Frequency Integrated
384 Circuits, Chap. 8, Cambridge University Press, New York
385 U.S.A. (1998).
- 386 [13] E. Sackinger et al., A 3-GHz 32-db CMOS limiting amplifier
387 for SONET OC-48 receiver, IEEE J.Solid-State Circ. 35
388 (2000) 1884.
- 389 [14] D. Guo et al., The 120Gbps VCSEL array based optical
390 transmitter (ATx) development for the High-Luminosity LHC
391 (HL-LHC) experiments, Journal of Instrumentation, 2014
392 JINST 9 C02007.
- 393 [15] Samtec Ltd, Ultra Low Profile Micro Array Z-Ray Catalog, F-
394 215 Rev 22JUL15.
- 395 [16] R. King et al., Commercial VCSELs and VCSEL arrays
396 designed for FDR (14 Gbps) optical links, Vertical-Cavity
397 Surface-Emitting Lasers XVI, Proc.SPIE, 2012 8276, 82760G.